Hindawi
Journal of Nanomaterials
Volume 2022, Article ID 7604383, 16 pages
https://doi.org/10.1155/2022/7604383

Research Article

Strength Prediction of Self-Consolidating Concrete Containing Steel Fibre with Different Fibre Aspect Ratio

Ganesh Prabhu Ganapathy,[1] **Lakshmi Keshav**,[2] **Gokulan Ravindiran**,[1] **and Nasar Ali Razack**[3]

[1]*Department of Civil Engineering, GMR Institute of Technology, Rajam, Andhra Pradesh, India*
[2]*Department of Civil Engineering, VR Siddhartha Engineering College, Vijayawada, Andhra Pradesh, India*
[3]*Department of Civil Engineering, College of Engineering and Technology, Samara University, afar, Ethiopia 7240*

Correspondence should be addressed to Nasar Ali Razack; nasar.ali01@su.edu.et

Received 15 February 2022; Revised 24 March 2022; Accepted 28 March 2022; Published 11 April 2022

Academic Editor: Samson Jerold Samuel Chelladurai

The present study presents the effects of steel fibre aspect ratio on the fresh and strength properties of self-consolidating concrete (SCC). Steel fibre having three different aspect ratios (50, 65 and 80) with the inclusion rate of 0.2%, 0.4%, 0.6%, 0.8%, and 1.0% was considered, and the effects of aspect ratio and the fibre inclusion rate on the fresh and strength properties of SCC were investigated. Central composite design (CCD) of RSM modeling was considered to propose a regression model to predict the 28-day compressive strength of SCC and steel fibre-reinforced SCC (SFSCC) incorporating different supplementary cementitious materials (SCMs). 94 data sets retrieved from various literatures and the experimental data set (SCC and SFSCC) of this present study have been used to develop the regression model. Further, cement content, powder content, water to binder ratio, and coarse aggregate to fine aggregate ratio were considered as basic variables to propose the model, and their influence on the strength properties of SCC was prioritized using analysis of variance (ANOVA) and Pareto chart. The findings of regression model have been compared with the results of 94 data sets, and the experimental data set of this present study and the comparisons confirm that the proposed regression model are very realistic and precise to predict the compressive strength of SCC and SFSCC with different aspect ratio.

1. Introduction

Self-consolidating concretes (SCC) is a flowing concrete that can be fill the formwork under its own weight without the need of any type of external vibration and compaction (El-Dieb and Reda Taha [1]). The hardened properties (both mechanical and durability) of the SCC are relatively similar to the conventional concrete. Because the cost associated with the consolidation of SCC is zero, the application of SCC in the construction industry becomes widespread. Because the occurrence of numerous seismic activities around the world, in recent years, the researchers started to show more interest to enrich the energy absorption capacity of the concrete structures (Doo-Yeol Yoo et al. [2]). Even though the SCC is stronger than the conventional concrete, the tensile strain capacity of the SCC is very poor under seismic loadings.

It has been well documented that the tensile strain capacity of the concrete can be enhanced by adding fibres both steel and synthetic fibres. Apart from other fibres, the potential utilization of steel fibres in concrete enhanced the structural performance of the determinate and indeterminate structures and also in practice for many years (Halit Cenan Mertol et al. [3]). Doo Yeol Yoo et al. [4, 5] found that influence of steel fibre on the initial cracking strength of the concrete was negligible, however, significantly controlled the post cracking strength of the concrete. The emerging of fibre-reinforced self-consolidating concretes (FRSCC) extends the application of SCC in higher end structural applications and includes densely reinforced elements such as floors, walls, precast elements, and offshore structures (Alberti et al. [6]). It is well recognized that the inclusion/addition of fibre in SCC affects the workability and flow characteristics of fresh concrete, and the uniformity in the distribution of fibres is very imperative to achieve the optimum benefits of the fibre (Wijffels et al. [7]. The test results of Thiago Melo Grabois et al. [8] exhibited the same. In recent years, numerous researches have been performed to determine the influences of fibre on the flow properties and the strength properties of SCC. Mustafa Sahmaran et al. [9] reported that the fibre type, and fibre geometry (i.e., length and aspect ratio) and surface roughness of the fibres impaired the flow characteristic of the SCC. Sherif Yehia et al. (2018) recognized that the higher stiffness and the configuration of the steel fibre rise the friction between the aggregates and fibres and, thus, reduced the workability of SCC more than the synthetic fibre.

Though various researches have been performed to evaluate the influences of steel fibre on the flow and strength properties of SCC, more researches are needed to be performed to understand the influence of fibre aspect ratio on the flow and strength properties of SCC. With this intention, an experimental investigation was initiated to evaluate the influences of fibre aspect ratio on the flow and strength properties of SCC. The experimental parameters were fibre aspect ratio and fibre inclusion rate. Steel fibres with three aspect ratios (50, 65, and 80) were used in this study. Because the 28-day compressive strength of any concrete is essential for any structural design, tests are carried out at the age of 28 days to determine the compressive strength of any concrete. In few circumstances, due to some errors in the mix design, lacking in sample preparation and erroneous testing, the process of strength prediction has to be repeated which may led to increase in cost and timing (Rafat Siddique et al. (2011)). So it is imperative to develop a model to predict the 28-day compressive strength of steel fibre-reinforced SCC (SFRSCC). Over the past several decade, various researchers performed researches to establish a model to predict the strength of the concrete using neural network (Lee [10] and Sebastia et al. [11]). Using traditional regression analysis, over the past few decades, efforts have been made to predict the compressive strength properties. However, the development of model to predict the strength of SFSCC has not been investigated completely. In this present study, attempt was made to develop a regression model to predict the 28-day compressive strength of SFSCC. Because the preciseness of the regression chiefly depends on the number of data set, 94 mixture data sets have been retrieved from various literatures, and the regression model was developed. Further, the factors influencing the strength properties of SFSCC are also prioritized.

2. Experimental Program

2.1. Material Properties, Mix Proportions. For the SCC production, the ordinary Portland cement (OPC) was selected as a binding material. The binding material was tested according to the procedure recommended in [12] to evaluate the specific gravity, and the ascertained value was about 3.10.

Table 1: Chemical property of the cement.

	% by mass
Lime (as CaO)	62–64
Soluble silica (as SiO2)	19–20
Alumina (as Al2O3)	4.2–5.5
Iron oxide (as Fe2O3)	4.2–4.5
Magnesia (as MgO)	0.4–0.6
Sulfur calculated as sulfuric anhydride (as SO3)	2.2–2.5
Loss on ignition (LOI)	1.3–2.2

Chemical analysis test is also performed on binding material, and the obtained values are listed in Table 1. Industrial grade fly ash classified as grade C was obtained from Salem, Tamil Nadu, India, and was used in this study. The super plasticizer with the combination of hydroxyl-propyl methyl cellulose and poly-carboxylic was used in this study to enhance the flow properties of the SCC. Locally available river sand with the grain size between 1 mm and 3 mm was used in this study as a fine aggregate. The coarse aggregate with the maximum aggregate size of 14 mm was used. Steel fibres having the length of 30 mm, 35 mm, and 60 mm were used in this study, and the diameter of the fibre was between 0.55 mm to 0.75 mm. The physical and mechanical properties of the steel fibre are summarized in Table 2.

The average slump flow of the plain SCC mixture was about 700 mm containing minimum cement content, and the employed water binder ratio was about 0.45. To ascertain the most favorable distribution of the aggregates, maximum dry packing density was obtained according to the procedure recommended in ASTM C29/29 M-09. With respect to that, the aggregate distribution was taken as 40% and 60% for coarse and fine aggregate, respectively. The proportions of the plain SCC mixture are detailed in Table 3.

2.2. Specimen Preparation and Testing. The SCC mixtures were prepared with and without the substitution of steel fibres, and the inclusion rate of steel fibre was 0.2%, 0.4%, 0.6%, 0.8%, and 1.0%. Steel fibre having an aspect ratio of 64 and 73 was used in this study to improve the tensile strength properties of SCC. The concrete cubes with the size of 150 mm × 150 mm × 150 mm were used to test the compressive strength of the concrete mixture, and the compressive testing machine with the capacity of 2000 kN was used to perform the test. The cylinders (150 mm × 300 mm) and prisms (100 mm × 100 mm × 500 mm) were cast to test the tensile and flexural strength of the concrete mixtures. The flexural testing machine with the capacity of 500 kN was used to test the prisms. The counter current mixer was used to prepare all the concrete mixture, and the casting was done at room temperature. After casting, the specimens were demolded after 24 hours, and the specimens were subjected to curing until the testing.

3. Results and Discussion

3.1. Fresh Concrete Properties. The test was performed to evaluate the influences of the fibre and its aspect ratio on

Table 2: Physical and mechanical properties of fibres.

Fibre type	Density of the fibre (kg/m^3)	Diameter of the steel fibre (mm)	Length of fibre (mm)	Aspect ratio of the fibre	Modulus of elasticity (N/mm^2)	Tensile strength (N/mm^2)	Anchorage	Surface texture
Steel fibre–crimped and hooked	7850	0.55	30	55	200000	1100	Hooked	Smooth
		0.55	35	65		1150		
		0.75	60	80		1100		

Table 3: Mixture proportions.

Material description	Quantity/M^3
Cement	247 kg
Fly ash	157 kg
Natural sand	856 kg
Coarse aggregate (5 mm to 9 mm)	448 kg
Coarse aggregate (10 mm to 14 mm)	448 kg
Water/binder ratio	0.45
Super plasticizer	0.80% of cement mass

the fresh state properties of the SCC. To ascertain the fresh state properties of fibre-modified SCC, slump flow and V-funnel test were performed, and the tests were performed according to the procedure described in the EN: 12350-8 [13] and EN: 12350-9 [14], respectively. As shown in Figures 1–3, the inclusion of steel fibre into the fresh concrete results in a significant reduction in workability; furthermore, the increase in the fibre content reduced the workability further.

The decrease in the fresh concrete properties with respect to the fibre inclusion is presented in Figures 1–3. The slump flow spread of the reference mixture was about 690 mm, whereas the mixtures FRSCC-55-0.2%, FRSCC-55-0.4%, FRSCC-55-0.6%, FRSCC-55-0.8%, and FRSCC-55-1.0% achieved a slump flow spread of 674 mm, 651 mm, 631 mm, 604 mm, and 574 mm, respectively, which are 2.39%, 5.99%, 9.35%, 14.23%, and 20.09%, respectively, lower than the reference mixture. With respect to V-funnel test, the SCC with steel fibre showed higher emptying times; in addition, the increase in fibre content increased emptying time further. However, the values obtained were within the optimum values. As shown in Figure 1, the increase in the aspect ratio of the fibre exhibits a flow reduction in SCC; however, the reduction was not significant, and the obtained observation concurred with the findings of Son Yap et al. [15]. For instance, the mixture FRSCC-55-1.0% achieved a slump spread of 550 mm, whereas the mixture FRSCC-65-1.0% and FRSCC-80-1.0% exhibited a slump spread of 531 mm and 519 mm, which are 3.57% and 5.97% lower than the FRSCC-55-1.0%. The similar observation was observed in V-funnel test as well. When compared to mixture FRSCC-55-1.0%, the mixture FRSCC-80-1.0% showed 14.01% higher emptying time. Because the formation of fibre-cement matrix network and the density is proportional to the fibre aspect ratio, the reduction in fresh state properties was observed with respect to increase in the fibre aspect ratio.

3.2. Mechanical Properties

3.2.1. Compressive Strength. The test results concerning with the compressive strength development of SFSCC mixture for all ages are presented in Figures 4 and 5. From Figures 4 and 5, it can be seen that there was a moderate enhancement (ranges from 4% to 5% enhancement) in compressive strength which was observed with the increase in steel fibre inclusion rate in all ages.

For instance, the 28-day compressive strength of the concrete mixtures FRSCC-55-0.2%, FRSCC-55-0.4%, FRSCC-55-0.6%, FRSCC-55-0.8%, and FRSCC-55-1.0% was 38.92 N/mm^2, 39.12 N/mm^2, 39.65 N/mm^2, 40.01 N/mm^2, and 40.12 N/mm^2, respectively, which are 4.81%, 5.41%, 6.82%, 7.81%, and 811% higher than that of CM. The enhancement in the compressive strength of the SFSCC is solely attributed to the addition of steel fibre. The crack arresting ability or bridging effect of the fibre led to the increase in the compressive strength of the SFSCC. In addition, because of the bridging effect of the fibre, the cubes with steel fibre exhibited more ductile failure (complete specimen damage) instead of sudden catastrophic failure.

The increase in the aspect ratio of the fibre did not increase the compressive strength of SCC considerably; moreover, approximately 2% of enhancement in compressive strength was observed. For instance, at the age of 28 days, FRSCC-55-0.6% achieved a strength of 39.65 N/mm^2, whereas the specimens FRSCC-65-0.6% and FRSCC-80-0.6% achieved a strength of 39.85 N/mm^2 and 40.12 N/mm^2, respectively, which are 0.05% and 1.48%, respectively, higher than the FRSCC-55-0.6%. As discussed earlier, in compression test, the dispersed fibre in the concrete reduced the crack tip stress concentration and acted as a crack arrester. Though the increase in the aspect ratio of the fibre enhanced the bridging/anchorage effect of the concrete, a very minimum enhancement in the compressive strength was observed. However, the aspect ratios of the fibre made the cube specimens become more intact.

3.2.2. Split Tensile and Flexural Strength. The 7-, 28-, and 90-day split tensile strength of all mixtures are presented in Figures 6 and 7, respectively. Unlike compressive strength, the presence of steel fibre improved the tensile strength properties of SCC, and the increase in the quantity of steel fibre enhanced the SCC tensile strength further. The enhancement in tensile of the SCC obtained with the

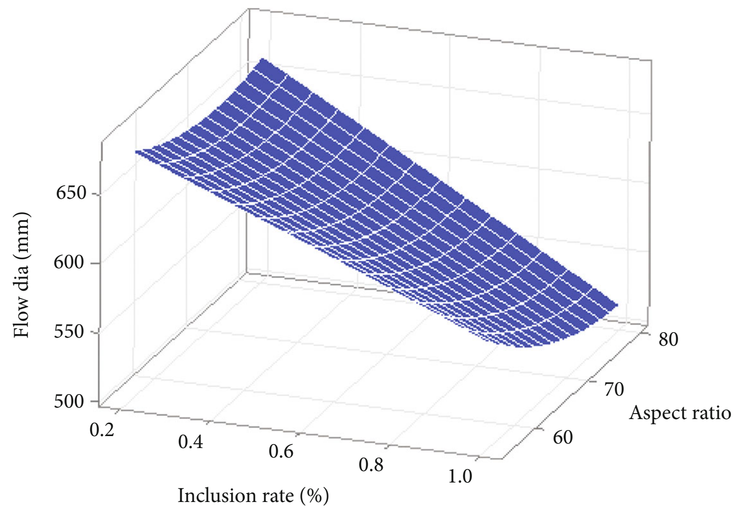

Figure 1: Effect of fibre inclusion and the increase in aspect ratio on slump flow spread.

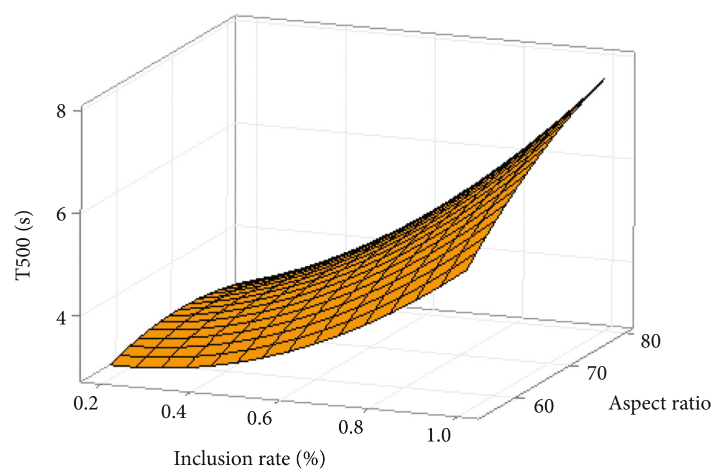

Figure 2: Effect of fibre inclusion and the increase in aspect ratio on T_{500}.

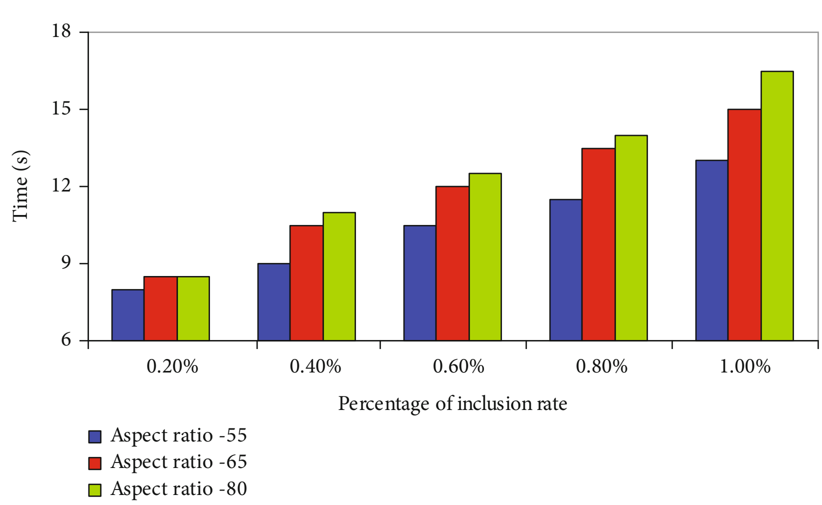

Figure 3: Effect of fibre inclusion and the increase in aspect ratio on emptying time of V-funnel test.

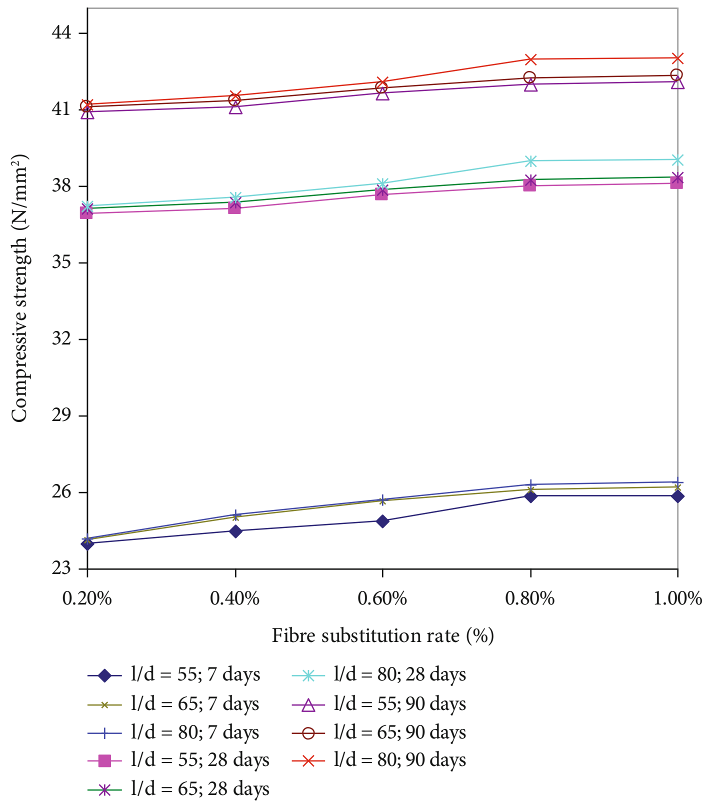

Figure 4: Effect of fibre inclusion and the increase in aspect ratio on compressive strength of SCC–comparison.

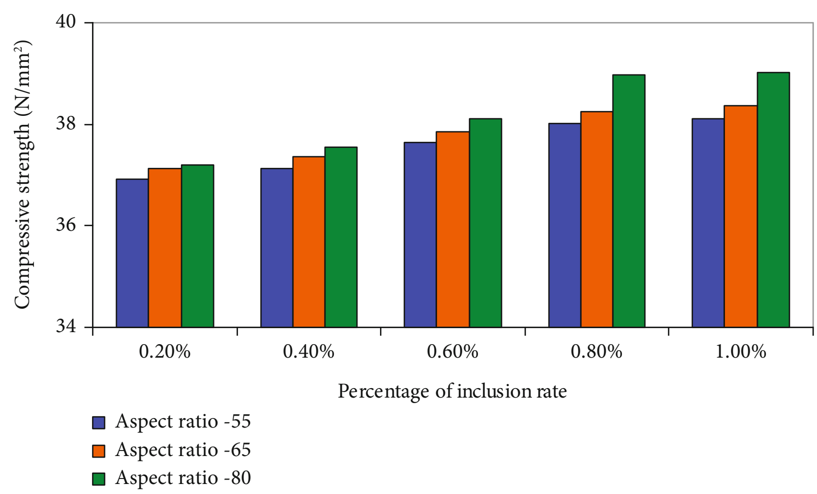

Figure 5: Effect of fibre inclusion and the increase in aspect ratio on 28-day compressive strength of SCC–comparison.

inclusion of steel fibre may due to the bridging/anchorage effect of the fibres and the higher modulus of elasticity of the steel fibre. At the age of 28 days, compared to CM, the increase in tensile strength of the concrete mixtures FRSCC-55-0.2%, FRSCC-55-0.4%, FRSCC-55-0.6%, FRSCC-55-0.8%, and FRSCC-55-1.0% was about 5.11%, 7.29%, 15.05%, 19.35%, and 21.50%, respectively.

The increase in the aspect ratio exhibited pronounced effect on the tensile strength of the SCC; in addition, the increase in the inclusion rate enhanced the tensile strength further (see Figure 7). For instance, the specimen FRSCC-65-0.6% and FRSCC-80-0.6% exhibited a tensile strength of 4.28/mm^2 and 4.31 N/mm^2, respectively, and enhanced their tensile strength by 3.92% and 4.86%, respectively, than that of FRSCC-55-0.6% which achieved a tensile strength of 4.12 N/mm^2. Since the aspect ratio of fibre is high, the bridging/anchorage developed by the fibre and the tensile stress developed by the fibre were increased during the applied load. The flexural strength of FRSCC is presented in Figures 8 and 9. Like split tensile strength, the flexural strength of SCC

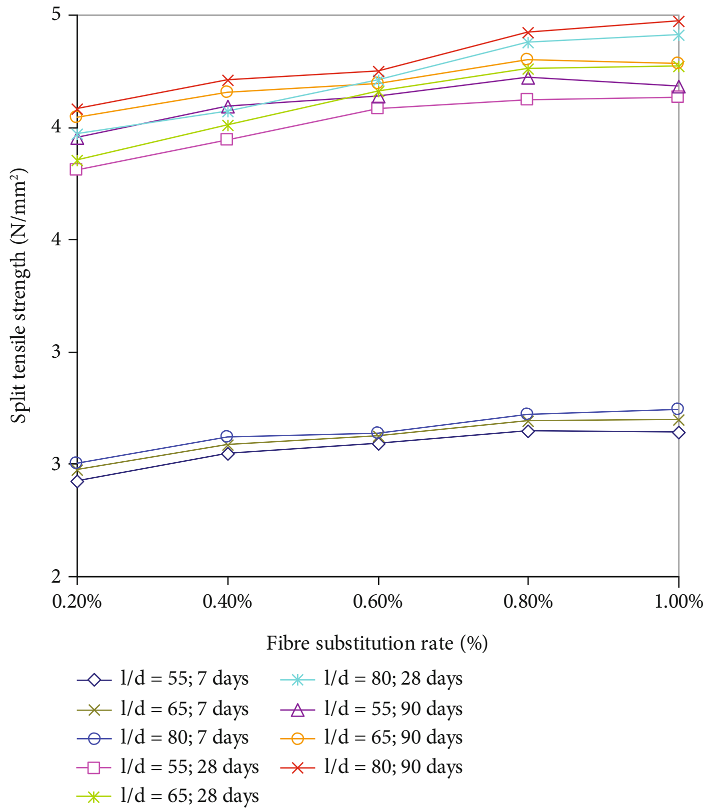

Figure 6: Effect of fibre inclusion and the increase in aspect ratio on split tensile strength of SCC–comparison.

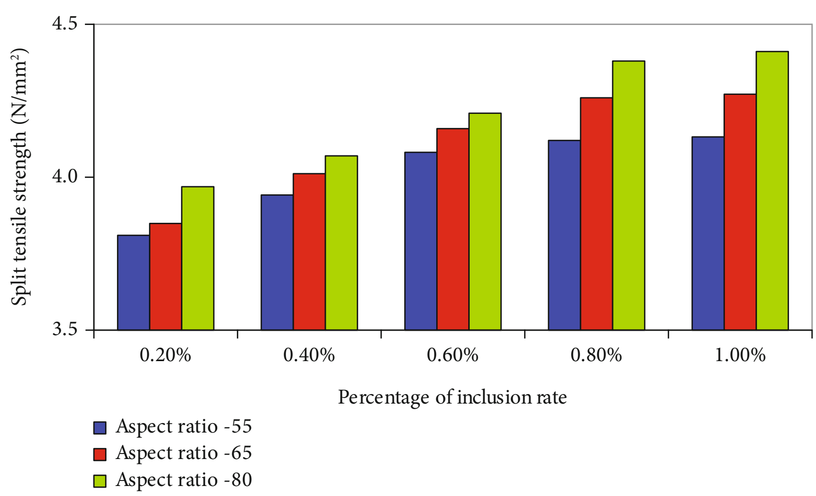

Figure 7: Effect of fibre inclusion and the increase in aspect ratio on 28-day split tensile strength of SCC–comparison.

enhanced with the inclusion of SCC, and further enhancement in strength was observed with increase in the inclusion rate. However, beyond the inclusion rate of 0.80%, there was no significant enhancement in the flexural strength observed.

4. Compressive Strength Prediction of Self-Consolidating Concretes

4.1. Background. In the new era, the introduction of SCC has fetched numerous technological advancements in the construction industry. Further, the utilization of SCMs in SCC has reduced the CO_2 emission and improved the bleeding, flow ability, and finishing capability of the SCC. Compressive strength at the age 28 days is the most important property of SCC, and this value is widely used for structural design calculation. It is well documented that the prediction of 28-day compressive strength of an SCC is very imperative in the modern construction industry for better engineering predictions. Generally the compressive strength SCC is evaluated through experimental tests. Over the past several

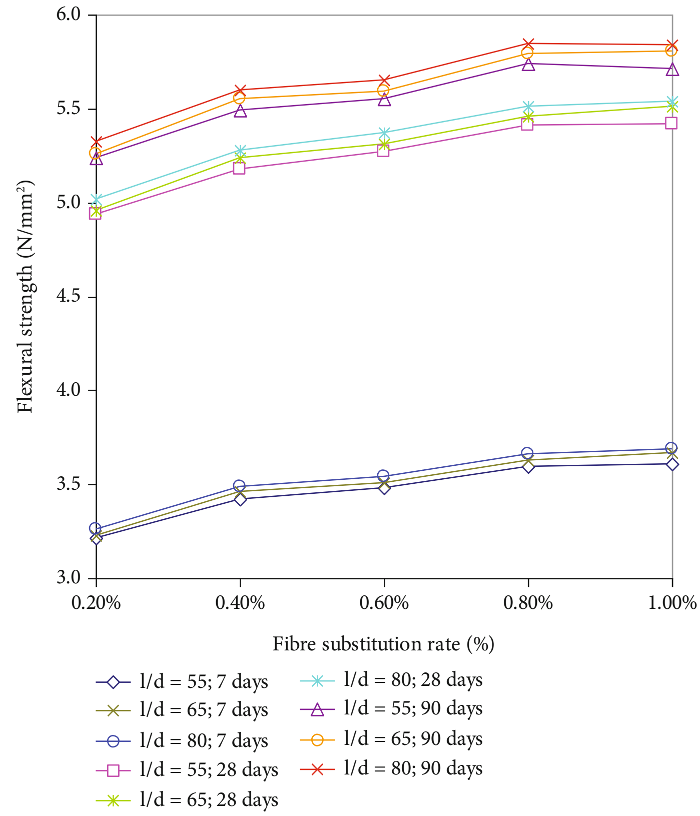

Figure 8: Effect of fibre inclusion and the increase in aspect ratio on flexural strength of SCC–comparison.

decades, few of the statistical models were proposed to determine the compressive strength of SCC and the key factor that influence the strength of the SCC considered as water to binder ratio and the ingredients added to the SCC. Recently, Alyhya [16] proposed a simple model to predict the compressive strength of a SCC using regression analysis, and the water to binder ratio was considered as a key influential factor.

$$\mathrm{CS28} = \frac{195}{12.65^{w/b}}, \tag{1}$$

where W/B is the water to binder ratio. Based on the 204 test results available in the various literatures, Panagiotis G. Asteris et al. [17] developed a model (Equation (3)) to predict the 28-day compressive strength of SCC containing metakaolin as a SCM. Multivariate adaptive regression splines (MARS) and M5P MT are used to develop a model and to establish key factors that influence strength of SCC.

$$\mathrm{CS}_{28} = f\left(C, \mathrm{MK}, B, \mathrm{SP}, \frac{\mathrm{CA}}{\mathrm{FA},}, D_{\max}\right), \tag{2}$$

where C, MK, and SP are the cement (Kg/m^3), metakaolin (Kg/m^3), and super plasticizer (Kg/m^3), respectively, and CA/FA and W/B are the coarse aggregate to fine aggregate ratio and water to binder ratio, respectively. $D_{\max}$ is the maximum size of the aggregate used to prepare the concrete. Using six rules in M5P model tree method, seven inputs and one output parameter were employed to predict the 28-day strength of SCC. The model developed using six rules is provided in Equations (1)–(2). The finding of model proposed by Panagiotis G. Asteris et al. [17] was shown superior predictions than the Alyhya [16]; further, the "coefficient of R^2" of the model was above 92%.

$$\begin{aligned}
&SP \le 4.316\\
&\quad SP \le 1.26\\
&\quad W/B \le 0.44(-0.009 * B + 1.95 * SP + 5.99 * CA/FA - 5.045 * W/B + 38.63),\\
&\quad W/B > 0.44(-0.009 * B + 1.95 * SP + 8.38 * CA/FA - 72.64 * W/B + 60.99),\\
&\quad SP > 1.26\\
&CA/FA \le 0.971\begin{pmatrix} 0.06 * C + 0.10 * MK - 0.051 * B + 3.53 * SP - 5.56 * CA/FA \\ -76.13 * W/B + 63.81 \end{pmatrix},\\
&CA/FA > 0.971\begin{pmatrix} 0.031 * MK - 0.025 * B + 2.97 * SP + 9.94 * CA/FA \\ -12.15 * W/B + 46.79 \end{pmatrix},\\
&\quad SP > 4.316\\
&CA/FA \le 1.03\begin{pmatrix} 0.032 * MK - 0.02 * B + 1.18 * SP - 15.82 * CA/FA \\ -3.99 * W/B + 74.96 \end{pmatrix},\\
&CA/FA > 1.03\begin{pmatrix} 0.035 * C - 0.027 * MK + 2.74 * SP + 6.94 * CA/FA \\ +32.68 * W/B + 25.2 \end{pmatrix}.
\end{aligned} \tag{3}$$

Víctor Revilla-Cuesta et al. [18] developed a complex regression model (Equation (4)) to predict the 28-day compressive strength of SCC. The age of the concrete and the percentage of fine recycled aggregate were considered as a

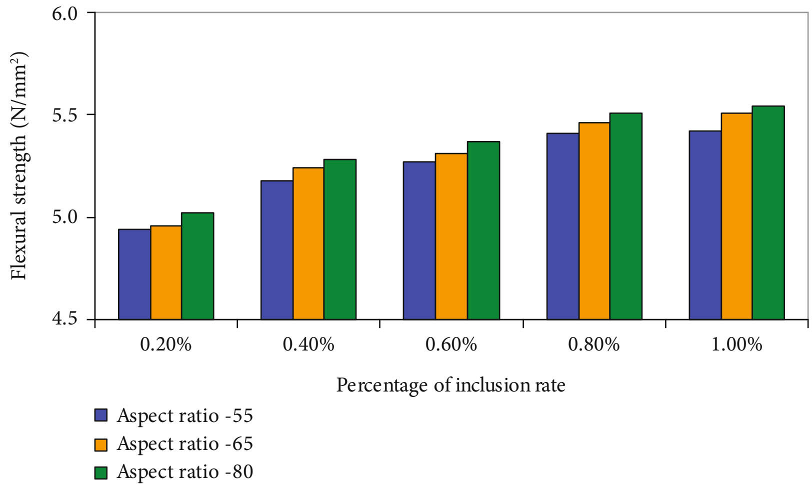

FIGURE 9: Effect of fibre inclusion and the increase in aspect ratio on 28-day flexural strength of SCC–comparison.

process variable to develop of strength prediction model. The model is not a general one, and it is limited to forecast the behavior of SCC with the strength ranging from 40 MPa to 60 MPa.

$$\mathrm{CS} = 26.7876 + \frac{1}{0.0284 + (0.0233/A)} - 0.2657.\mathrm{FRP} + 0.0005.A.(\mathrm{FRP} + 0.8373), \tag{4}$$

where A and FRP are the age of concrete and inclusion rate of fine recycled aggregate particles, respectively. Over the past few decades, a few more models were proposed to predict the strength of the SCC; though, researches need to be performed to develop a model to predict the compressive strength of steel fibre-reinforced SCC.

4.2. Experimental Database and Proposed Strength Prediction Model. Though few researches have been carried out on inclusion of steel fibre to enhance the strength properties of the SCC, it is very imperative to propose a simplified model to predict the 28-day compressive strength of an SCC containing steel fibre for better engineering decisions. In this present study, the central composite design (CCD) of RSM modeling was used to establish a model to predict the 28-day compressive strength of conventional SCC and the SCC containing steel fibre with different aspect ratio. Initially, the regression model was developed to predict the 28-day compressive strength of conventional SCC, followed by a regression model proposed to predict the 28-day compressive strength of SCC containing steel fibre with different aspect ratio. With respect to regression model, the preciseness of the models primarily depends on the number of data set that used develop the model. Further, large varieties of experimental data sets are needed to establish a relationship between process variables and the compressive strength of the SCC. A total of 94 mixture data sets (See Table 4) retrieved from various literatures were used in this study to propose a model and to predict the compressive strength of conventional SCC. Further, few of the data sets available in few studies have not been considered, because of the abstruseness in the mixture proportions and testing methods.

According to the test results obtained in this study and from various literatures, a simplified model is proposed (Equation ((5)) using regression analysis for predicting the 28-day compressive strength of conventional SCC in accordance with the unified theory approach. Cement content, powder content, water to binder ratio, and coarse aggregate to fine aggregate ratio were considered as basic variables to establish the model, and the super plasticizer dosage was considered as normal variable. Figure 10 exhibits the frequency histogram of the process variables.

$$\begin{aligned} SCC_{28} = {} & 332.5601 - (0.4864 \times W_c) - (0.9413 \times W_{FA}) \\ & - \left(436.4398 \times \left(\frac{W}{B}\right)\right) - \left(79.1974 \times \frac{CA}{FA}\right) \\ & + \left(0.0003 \times W_c^2\right) + \left(0.0006 \times W_{FA}^2\right) \\ & + \left(93.3578 \times \left(\frac{W}{B}\right)^2\right) - \left(56.7889 \times \left(\frac{CA}{FA}\right)^2\right) \\ & + (0.0013 \times W_c \times W_{FA}) + \left(0.2955 \times W_c \times \left(\frac{W}{B}\right)\right) \\ & + \left(0.1469 \times W_c \times \left(\frac{CA}{FA}\right)\right) + \left(0.3828 \times W_{FA} \times \left(\frac{W}{B}\right)\right) \\ & + \left(0.3085 \times W_{FA} \times \left(\frac{CA}{FA}\right)\right) \\ & + \left(133.9685 \times \left(\frac{W}{B}\right) \times \left(\frac{CA}{FA}\right)\right) \end{aligned} \tag{5}$$

where W_c and W_{FA} are the weight of cement and powder, respectively; W/B and CA/FA are the water to binder ratio and coarse aggregate to fine aggregate, respectively. The appropriateness and the fit of the model can be verified through predicted R^2 and adjustable-R^2; further, the difference between the adjustable-R^2 and predicted R^2 should be less than 20% (Jingfeng Wang et al. [23]). The difference between the predicted R^2 and the adjustable-R^2 of the

Table 4: Specification of data sets retrieved from various literatures.

	Cement (kg)	Powder (kg)	W/B	SP (%)	Sand (kg)	CA (kg)	CA/FA	$SCC_{28,exp}$ (MPa)	$SCC_{28,pred}$ (MPa)	$SCC_{28,exp}$/ $SCC_{28,pred}$
Sonebi [19, 20]	290	100	0.45	0.8	913	837	0.9168	42.70	46.87	0.911003464
	250	261	0.55	0.5	478	837	1.7510	17.00	15.03	1.131245483
	210	100	0.65	0.8	910	837	0.9198	19.10	19.75	0.967194856
	250	160	0.55	0.5	742	837	1.1280	24.10	27.60	0.873092269
	210	220	0.45	0.8	786	837	1.0649	26.70	34.58	0.772182383
	290	100	0.65	0.2	709	837	1.1805	26.60	19.52	1.362871229
	290	220	0.45	0.2	625	837	1.3392	32.90	41.36	0.795395955
	250	160	0.55	0.5	742	837	1.1280	26.00	27.60	0.94192527
	250	160	0.55	0.5	742	837	1.1280	28.50	27.60	1.032495007
	250	160	0.55	0.5	742	837	1.1280	26.40	27.60	0.956416428
	250	160	0.55	0	739	837	1.1326	27.30	27.38	0.996928631
	210	100	0.45	0.2	1066	837	0.7852	54.30	49.06	1.106830181
	317	160	0.55	0.5	594	837	1.4091	29.10	27.25	1.067704419
	250	29	0.55	0.5	1006	837	0.8320	51.70	41.38	1.249482816
	210	220	0.65	0.2	562	837	1.4893	10.20	9.30	1.097362823
	250	160	0.55	0.5	742	837	1.1280	25.30	27.60	0.916565743
	250	160	0.38	0.5	919	837	0.9108	48.30	50.97	0.947532872
	250	160	0.55	1	746	837	1.1220	26.70	27.89	0.957381832
	250	160	0.72	0.5	566	837	1.4788	11.00	6.55	1.679781079
	183	160	0.55	0.5	891	837	0.9394	22.10	24.37	0.906988063
Bouzoubaa and Lachemi [21]	247	165	0.45	0.12	845	846	1.0012	34.60	39.93	0.86648597
	238	159	0.4	0.29	844	844	1.0000	37.80	42.94	0.880289726
	232	155	0.35	0.38	846	847	1.0012	48.30	47.29	1.02128933
	207	207	0.45	0.4	845	843	0.9976	33.20	35.64	0.931481102
	200	200	0.4	0.17	842	843	1.0012	34.90	38.27	0.911957846
	197	197	0.35	0.28	856	856	1.0000	38.90	42.75	0.909927462
	169	254	0.45	0	853	853	1.0000	30.20	30.57	0.987945608
	163	245	0.4	0.2	851	851	1.0000	26.20	32.83	0.798045021
	161	241	0.35	0.3	866	864	0.9977	35.80	37.10	0.965012352
Hassan et al. [22]	400.1	49.5	0.4	0.8	921	891	0.9674	41.30	55.54	0.743628657
	414	36	0.4	0.8	923	893	0.9675	45.60	55.33	0.824090092
	427.5	22.5	0.4	0.8	926	896	0.9676	41.90	54.95	0.762521516
	436.5	13.5	0.4	0.8	927	898	0.9687	37.90	54.54	0.694884056
	450	0	0.4	0.8	930	900	0.9677	40.20	53.99	0.744638269
	436.5	13.5	0.4	0.8	929	899	0.9677	39.40	54.61	0.721487845
	427.5	22.5	0.4	0.8	928	898	0.9677	42.60	54.94	0.775325335
	414	36	0.4	0.8	926	897	0.9687	45.60	55.26	0.825214982
	400.5	49.5	0.4	0.8	925	895	0.9676	43.90	55.56	0.790119676
	382.5	67.5	0.4	0.8	923	893	0.9675	45.90	55.65	0.824831428
	360	90	0.4	0.8	921	891	0.9674	48.90	55.39	0.882832825
	337.5	112.5	0.4	0.8	919	889	0.9674	48.90	54.73	0.893533915

Table 4: Continued.

	Cement (kg)	Powder (kg)	W/B	SP (%)	Sand (kg)	CA (kg)	CA/FA	$SCC_{28,exp}$ (MPa)	$SCC_{28,pred}$ (MPa)	$SCC_{28,exp}/SCC_{28,pred}$
Patel et al. (2004)	220	180	0.39	0.35	916	900	0.9825	49.00	42.79	1.145260829
	160	240	0.39	0.35	886	900	1.0158	44.00	32.35	1.359971554
	193	158	0.39	0.35	1024	900	0.8789	44.00	45.78	0.961157989
	220	180	0.45	0.35	850	900	1.0588	38.00	33.65	1.129221416
	198	232	0.34	0.2	874	900	1.0297	46.00	42.92	1.071754467
	248	203	0.39	0.35	808	900	1.1139	50.00	42.21	1.184609709
	237	133	0.36	0.2	1034	900	0.8704	49.00	55.09	0.889441138
	220	180	0.39	0.35	916	900	0.9825	49.00	42.79	1.145260829
	237	133	0.43	0.5	960	900	0.9375	46.00	43.08	1.067704348
	275	155	0.43	0.5	827	900	1.0883	48.00	40.71	1.179046538
	280	120	0.39	0.35	946	900	0.9514	45.00	50.74	0.886941799
	170	200	0.43	0.2	930	900	0.9677	31.00	32.40	0.956933854
	220	180	0.39	0.6	916	900	0.9825	43.00	42.79	1.005024809
	220	180	0.39	0.35	916	900	0.9825	47.00	42.79	1.098515489
	220	180	0.39	0.1	916	900	0.9825	44.00	42.79	1.028397479
	198	232	0.39	0.5	872	900	1.0321	54.00	38.67	1.396539348
	220	180	0.39	0.35	916	900	0.9825	45.00	42.79	1.051770149
	220	180	0.33	0.35	982	900	0.9165	57.00	52.64	1.082894949
	170	200	0.43	0.5	928	900	0.9698	33.00	32.30	1.021628092
	275	155	0.43	0.2	830	900	1.0843	36.00	40.93	0.879462111
Ghezal and Khayat (2001)	325	60	0.65	0.43	899	850	0.9455	30.80	29.64	1.039211938
	325	60	0.65	0.43	899	850	0.9455	32.60	29.64	1.099945103
	325	120	0.75	0.43	755	850	1.1258	32.20	31.62	1.018316573
	249	60	0.68	0.43	1079	850	0.7878	24.00	24.72	0.970765292
	325	60	0.85	0.43	722	850	1.1773	13.30	14.94	0.89002298
	370	96	0.57	0.25	833	850	1.0204	39.50	43.49	0.908236051
	400	60	0.63	0.43	718	850	1.1838	30.40	31.96	0.951172049
	325	60	0.65	0.43	899	850	0.9455	35.30	29.64	1.191044851
	370	24	0.69	0.62	770	850	1.1039	18.70	21.63	0.864433584
	325	1	0.55	0.43	1042	850	0.8157	41.20	43.79	0.940878454
	280	96	0.87	0.25	820	850	1.0366	19.60	15.95	1.228836884
	325	60	0.65	0.75	896	850	0.9487	27.20	29.53	0.921034649
	325	60	0.65	0.43	898	850	0.9465	35.00	29.60	1.182321851
	325	60	0.65	0.12	900	850	0.9444	31.40	29.67	1.058211271
	370	96	0.57	0.62	830	850	1.0241	38.80	43.36	0.894794457
	325	60	0.65	0.43	898	850	0.9465	34.30	29.60	1.158675414
	280	96	0.87	0.62	817	850	1.0404	15.90	15.91	0.999210375
	370	24	0.69	0.25	772	850	1.1010	26.40	21.78	1.212328434

Table 4: Continued.

	Cement (kg)	Powder (kg)	W/B	SP (%)	Sand (kg)	CA (kg)	CA/FA	$SCC_{28,exp}$ (MPa)	$SCC_{28,pred}$ (MPa)	$SCC_{28,exp}/SCC_{28,pred}$
Bui et al. (2001)	350	162	0.59	0.009	768	840	1.0938	51.70	51.43	1.005171801
	349	162	0.57	0.14	779	852	1.0937	59.90	51.50	1.163206529
	350	133	0.52	0.16	815	883	1.0834	55.30	46.73	1.183516974
	350	111	0.51	0.15	831	900	1.0830	61.00	42.98	1.419196298
	250	257	0.77	0.11	787	853	1.0839	51.50	47.87	1.075778044
	427	115	0.45	0.12	779	844	1.0834	59.40	61.43	0.966916244
	348	224	0.5	0.43	783	848	1.0830	58.60	70.00	0.837190537
	350	90	0.48	0.14	852	923	1.0833	46.50	41.36	1.124294258
	327	173	0.53	0.2	902	803	0.8902	61.60	53.44	1.152719513
	380	145	0.48	0.1	788	854	1.0838	73.50	57.50	1.278221193
	350	186	0.51	0.11	786	851	1.0827	70.40	59.58	1.181530343
	380	145	0.48	0.13	988	659	0.6670	65.60	63.24	1.037366758
	380	192	0.53	0.1	931	621	0.6670	67.80	66.68	1.016872768
	275	250	0.67	0.09	775	840	1.0839	54.50	53.21	1.024274427
Present study	247	157	0.45	0.2	856	896	1.0467	37.11	37.20	0.99761442
Mean										*1.0102*

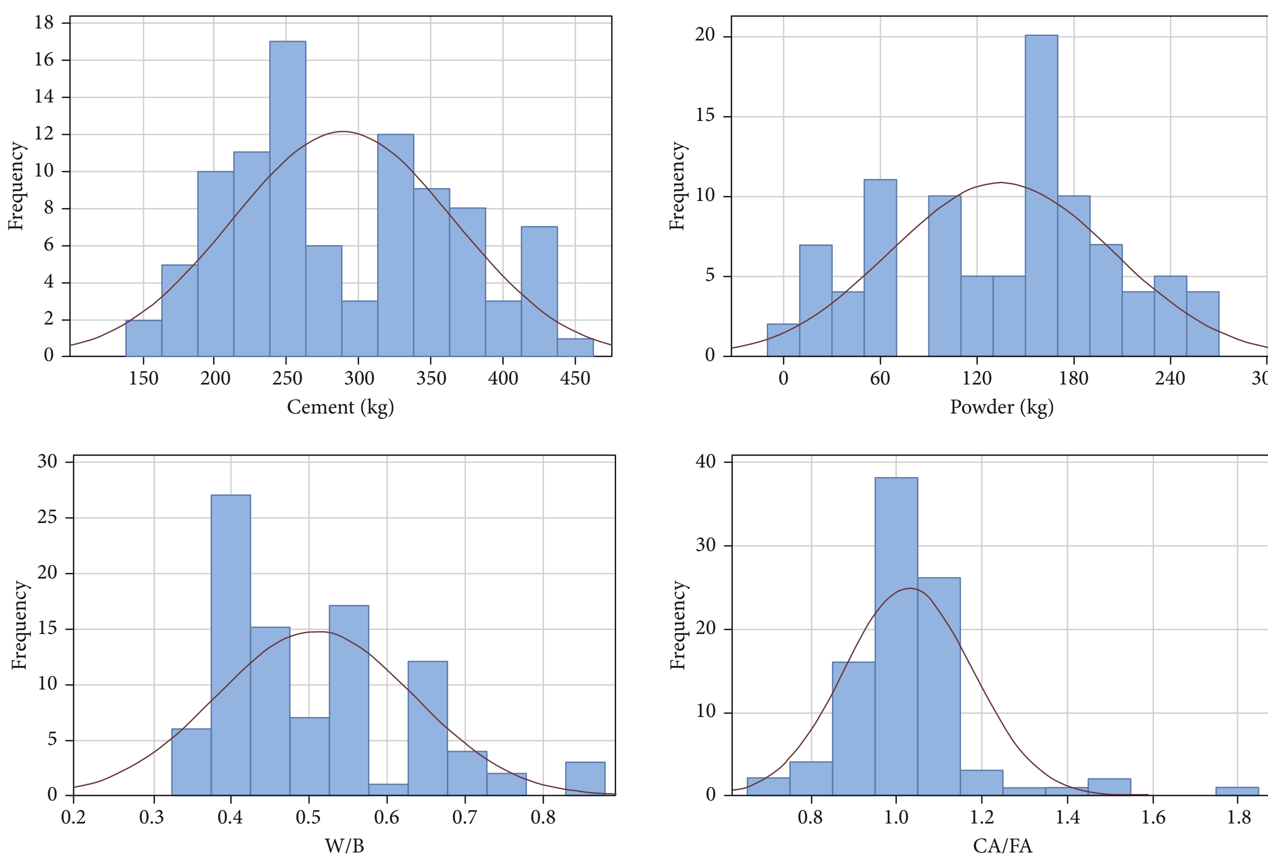

Figure 10: Histogram of the process variables.

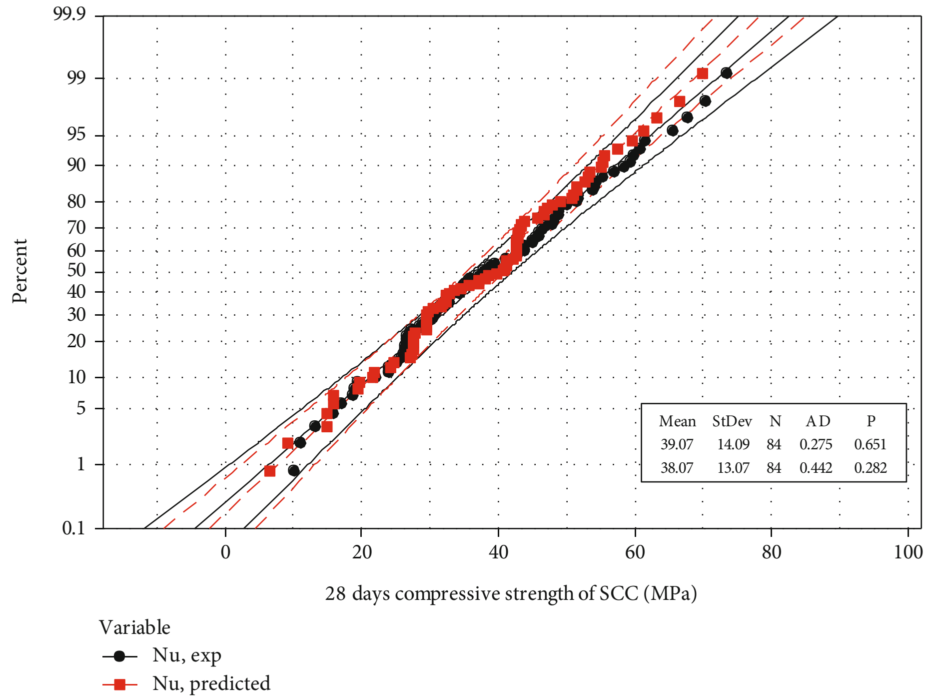

FIGURE 11: Validation of proposed model with data sets available in the literature-probability plot approach.

proposed model was less than 20%, revealing that the proposed model is very realistic; further, the R^2 value of the response SCC_{28} was 91.25, which is revealing that the 8.75% of variations only cannot be expressed by the proposed model.

Figure 11 shows the plot between the actual (94 mixture data sets) and the predicted strength of SCC at the age of 28 days, and it can be understood that the predicted compressive strength of the SCC is fairly in agreement with the experimental results; furthermore, the predicted strength was closely fit with the actual strength. It is well recognized that the model can be referred good, if the actual strength/predicted strength is very close or equal to 1.0. From the histogram (Figure 12), it can be visualized that most of the results (nearly 85% of results) falls in the range of 0.85 to 1.2, and very few results were fallen out of 0.8 and 1.2. This indicates that the proposed model is highly precise.

Analysis of variance (ANOVA) of CCD can be utilized to verify the relationship between the responses and the variables. The ANOVA of the regression analysis is listed in Table 5. Further, *P* value of the CCD also can be used to prioritize the influence of process variable as significance (<0.005) and highly significance (<0.001) on the response. From Table 5, it can be seen that the *P* value of the model is 0.0000, revealing that the proposed model of the present study is highly significant to predict the compressive strength SCC. As summarized in Table 5, *P* value of the cement, powder, and the CA/FA was 0.000, revealing that the parameters are highly significant. But the *P* value of the W/B was 0.0478, which is insignificant. Though the influence of cement, powder, and the CA/FA was significant, the effects of those variables on the compressive strength of SCC can be prioritized by Pareto bar chart. Figure 13 shows the Pareto chart of the compressive strength response. From Figure 13, it can be understood that the influence of cement is more significant than the other process variables, because the linear effect of cement is higher. Followed by cement, powder and CA/FA are more significant on the compressive strength of SCC.

With respect to the test results obtained in this study, a simplified model is proposed (Equation (6)) using regression analysis for predicting the 28-day compressive strength of steel fibre-reinforced SCC in accordance with unified theory approach. Steel fibre inclusion rate and fibre aspect were considered as basic variables to establish the model.

$$SFSCC_{28} = SCC_{28}\left(\begin{array}{c} 1.1209\text{-}\left(0.00265 \times \left(\dfrac{l}{d}\right)\right) - (0.0011 \times V_{\text{fibre}}) + \left(0.000021 \times \left(\dfrac{l}{d}\right)^2\right) \\ +\left(0.0008 \times V_{\text{fibre}} \times \left(\dfrac{l}{d}\right)\right) \end{array}\right), \tag{6}$$

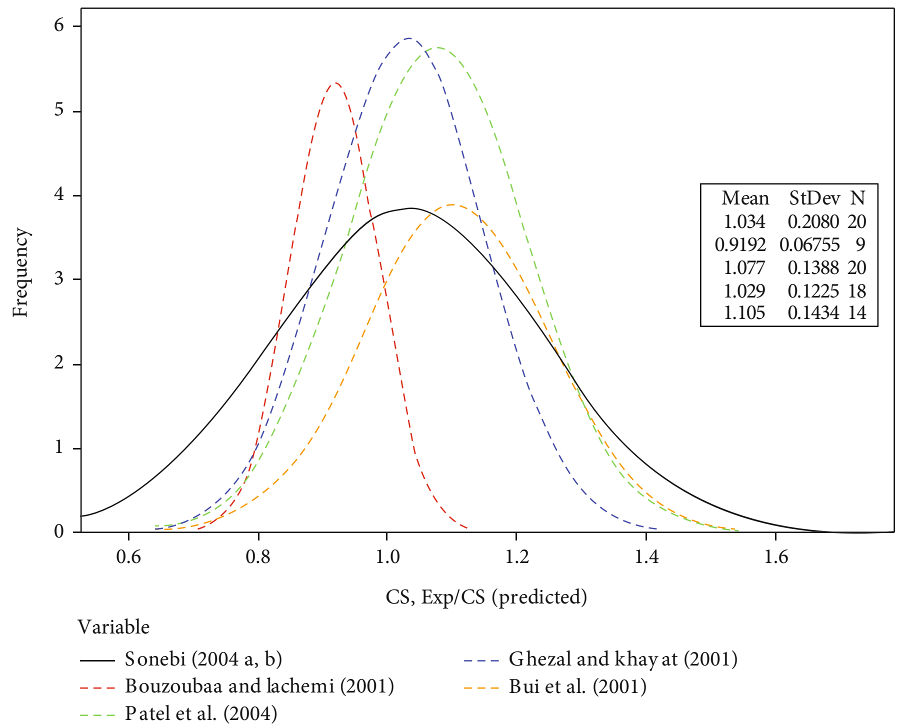

Figure 12: Validation of proposed model with data sets available in the literature–histogram approach.

Table 5: Analysis of Variance of SCC_{28}.

Source	DF	*F* value	*P* value
Model	14	30.98	≤0.001
Linear	4	32.22	≤0.001
Cement	1	61.77	≤0.001
Powder	1	37.76	≤0.001
W/B	1	0.44	0.508
CA/FA	1	25.70	≤0.001
Square	4	2.85	0.029
Cement∗cement	1	1.34	0.002
Powder∗powder	1	3.90	0.002
W/B∗W/B	1	1.38	0.244
CA/FA∗CA/FA	1	5.73	0.019
2-way interaction	6	9.47	≤0.001
Cement∗powder	1	13.64	≤0.001
Cement∗W/B	1	6.63	0.012
Cement∗CA/FA	1	1.21	0.005
Powder∗W/B	1	3.44	0.067
Powder∗CA/FA	1	5.22	0.005
W/B∗CA/FA	1	3.15	0.080
Lack-of-fit	67	8.42	≤0.001

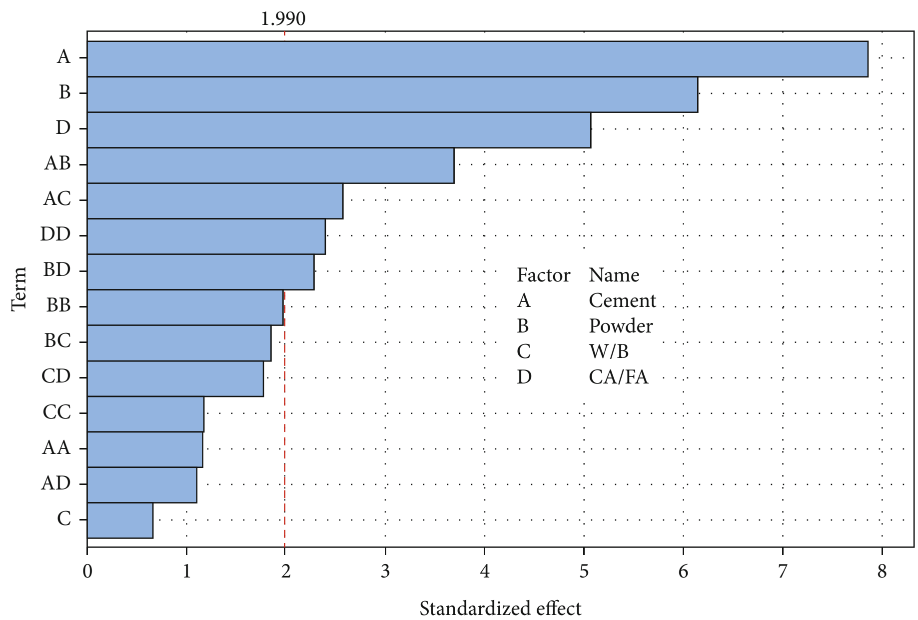

Figure 13: Influence of process variable on for SCC_{28}–Pareto chart.

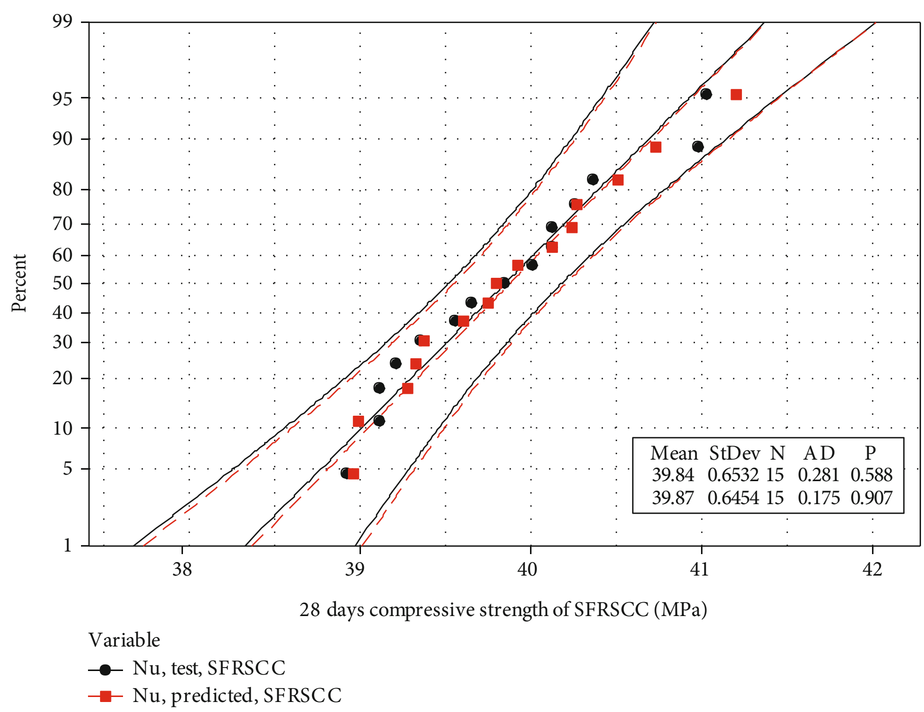

Figure 14: Validation of proposed model with present study test results–probability plot approach.

where V_{fibre} and l/d are the volume of fibre included (%) and steel fibre aspect ratio, respectively. The fit of the predicted strength to the experimental strength is presented in Figure 14.

From Figure 14, it can be understood that the predicted strength of the proposed model is in good agreement with the experimental strength. The mean of the actual/predicted strength is nearly 0.999, which is almost close to the experimental values. From the histogram (Figure 15), it can be visualized that most of the results are (nearly 95% of results) falling in the range of 0.98 to 0.99; very few results were fallen beyond the range of 0.98. This indicates that the proposed model is highly precise to predict the compressive strength of the SFSCC. The ANOVA of the regression analysis is provided in Table 6. From Table 6, it can be seen that the P value of the model was 0.0000, revealing that the proposed model is highly significant to predict the compressive strength steel fibre-reinforced SCC.

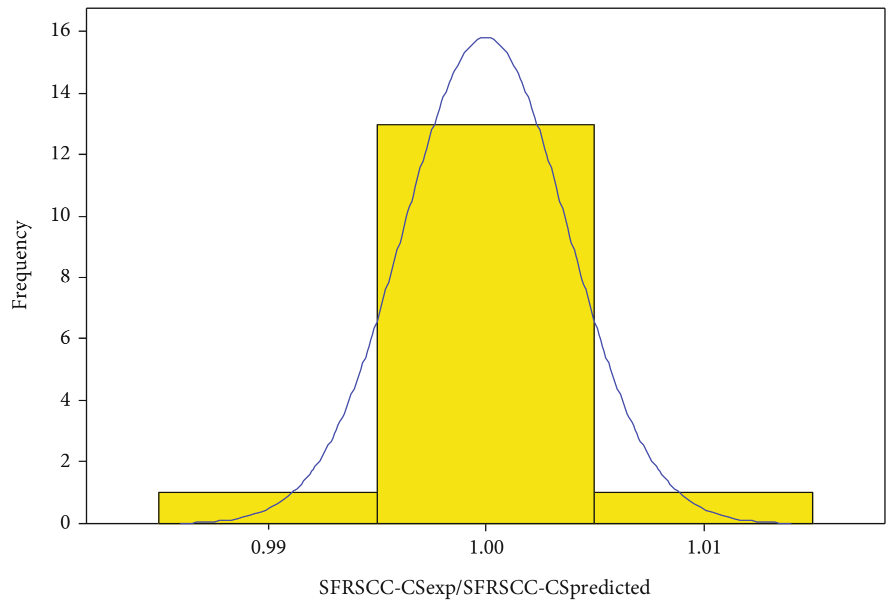

FIGURE 15: Validation of proposed model with present study test results–histogram approach.

TABLE 6: Analysis of Variance of $SFSCC_{28}$.

Source	DF	F value	P value
Model	5	47.62	≤0.001
Linear	2	116.87	≤0.001
Inclusion rate	1	194.50	≤0.001
Aspect ratio	1	39.25	≤0.001
Square	2	0.53	0.606
Inclusion rate∗inclusion rate	1	1.00	0.342
Aspect ratio∗aspect ratio	1	0.06	0.817
2-way interaction	1	7.18	0.025
Inclusion rate∗aspect ratio	1	7.18	0.025

5. Conclusion

In this present study, the fresh state properties and a strength property of the self-consolidating concretes (SCC) containing steel fibre with different aspect ratio have been investigated. Regarding the fresh state properties, the inclusion of steel fibre in SCC developed a fibre-cement matrix network and resulted in lower the flowability of the SCC; however, there was no segregation, and blockage was observed during the test. Though the flowability of the SCC reduced to the maximum of 20.09% with the steel fibre inclusion rate of 1%, the fresh state properties of the SFSCC mixtures were satisfied the threshold value recommended in most common standards. Because the formation of fibre-cement matrix network is directly related with the aspect ratio of fibre, the increase in the fibre aspect ratio lowered the flowability of the SCC. Though the presence of steel fibre was moderately enriched, the compressive strength of SCC significantly improved the tensile strength properties of the SCC. Further, the change in the fibre aspect ratio resulted in a 5% enhancement in tensile strength of the SCC. Central composite design (CCD) of RSM modeling has been considered to develop a regression model to predict the strength of SCC and SFSCC incorporated with different SCMs. To develop a regression model, 94 mixture data sets retrieved from various literatures were used. The findings of regression model have been compared with the results of 94 data sets and the experimental data set of this present study. The comparisons confirm that the proposed regression model is very realistic and precise to predict the compressive strength of SCC and SFSCC with different aspect ratio. The ANOVA and Pareto chart of the response revealed that the influence of cement is more significant than the other process variables, because the linear effect of cement is higher. Followed by cement, powder and CA/FA are more significant on the compressive strength of SCC.

Data Availability

The data used to support findings of this study are included within the article.

Disclosure

This study was performed as a part of the employment of Samara University, Ethiopia and GMR Institute of Technology, Rajam, Andhra Pradesh, India.

Conflicts of Interest

The authors declare that there are no conflicts of interest regarding the publication of this paper.

Acknowledgments

The authors appreciate the supports from Samara University, Ethiopia. The authors thank GMR Institute of Technology, Rajam, Andhra Pradesh for the technical assistance to complete this experimental work.

References

[1] A. El-Dieb and M. M. Reda Taha, “Flow characteristics and acceptance criteria of fibre-reinforced self-compacted concrete (FR-SCC),” *Construction and Building Materials*, vol. 27, no. 1, pp. 585–596, 2012.

[2] D. Y. Yoo, N. Banthia, S. W. Kim, and Y. S. Yoon, “Response of ultra-high-performance fibre-reinforced concrete beams with continuous steel reinforcement subjected to low-velocity impact loading,” *Composite Structures*, vol. 126, pp. 233–245, 2015.

[3] H. C. Mertol, E. Baran, and H. J. Bello, “Flexural behavior of lightly and heavily reinforced steel fibre concrete beams,” *Construction and Building Materials*, vol. 98, pp. 185–193, 2015.

[4] D.-Y. Yoo, Y.-S. Yoon, and N. Banthia, “Flexural response of steel-fibre-reinforced concrete beams: effects of strength, fibre content, and strain-rate,” *Cement and Concrete Composites*, vol. 64, pp. 84–92, 2015.

[5] D.-Y. Yoo, Y.-S. Yoon, and N. Banthia, “Flexural response of steel-fibre-reinforced concrete beams: Effects of strength, fibre content, and strain-rate,” *Cement and Concrete Composites*, vol. 64, pp. 84–92, 2015.

[6] A. G. Alberti, A. Enfedaque, J. C. Gálvez, and V. Agrawal, “Fibre distribution and orientation of macro-synthetic polyolefin fibre reinforced concrete elements,” *Construction and Building Materials*, vol. 122, pp. 505–517, 2016.

[7] M. J. H. Wijffels, R. J. M. Wolfs, A. S. J. Suiker, and T. A. M. Salet, “Magnetic orientation of steel fibres in self-compacting concrete beams: effect on failure behavior,” *Cement and Concrete Composites*, vol. 80, pp. 342–355, 2017.

[8] T. M. Grabois, G. C. Cordeiro, and R. D. T. Filho, “Fresh and hardened-state properties of self-compacting lightweight concrete reinforced with steel fibres,” *Construction and Building Materials*, vol. 104, pp. 284–292, 2016.

[9] M. Sahmaran, A. E. Yurtseven, and I. O. Yaman, “Workability of hybrid fibre reinforced self-compacting concrete,” *Building and Environment*, vol. 40, no. 12, pp. 1672–1677, 2014.

[10] S. Lee, “Prediction of concrete strength using artificial neural networks,” *Engineering Structures*, vol. 25, no. 7, pp. 849–857, 2003.

[11] M. Sebastia, I. F. Olmo, and A. Irabien, “Neural network prediction of unconfined compressive strength of coal fly ash–cement mixtures,” *Cement Concrete Reseach*, vol. 33, no. 8, pp. 1137–1146, 2003.

[12] I. Standard, *IS 8112: 2013: Ordinary Portland Cement, 43 Grade—Specification*, Bureau of Indian Standards, New Delhi, India, 2013.

[13] EN 12350–8, *Testing fresh concrete. Part 8: Self-compacting concrete*, Slumpflow test, 2010.

[14] EN 12350–9, *Testing fresh concrete. Part 9: Self-compacting concrete*, Vfunnel test, 2010.

[15] S. P. Yap, K. R. Khaw, U. Johnson Alengaram, and M. Z. Jumaat, “Effect of fibre aspect ratio on the torsional behaviour of steel fibre-reinforced normal weight concrete and lightweight concrete,” *Engineering Structures*, vol. 101, pp. 24–33, 2015.

[16] W. S. Alyhya, *Self-compacting concrete: mix proportioning, properties and its flow simulation in the V-funnel*, Doctoral Dissertation, Cardiff University, 2016.

[17] P. G. Asteris, A. Ashrafian, and M. Rezaie-Balf, “Prediction of the compressive strength of self-compacting concrete using surrogate models,” *Computers and Concrete*, vol. 24, no. 2, pp. 137–150, 2019.

[18] V. Revilla-Cuesta, M. Skaf, A. B. Espinosa, A. Santamaría, and V. Ortega-López, “Statistical approach for the design of structural self-compacting concrete with fine recycled concrete aggregate,” *Mathematics*, vol. 8, no. 12, p. 2190, 2020.

[19] M. Sonebi, “Application of statistical models in proportioning medium strength self-consolidating concrete,” *ACI Material Journal*, vol. 101, no. 5, pp. 339–346, 2004.

[20] M. Sonebi, “Medium strength self-compacting concrete containing fly ash: modelling using factorial experimental plans,” *Cement Concrete Research*, vol. 34, no. 7, pp. 1199–1208, 2004.

[21] N. Bouzoubaa and M. Lachemi, “Self-compacting concrete incorporating high volumes of class F fly ash: preliminary results,” *Cement Concrete Research*, vol. 31, no. 3, pp. 413–420, 2001.

[22] A. A. A. Hassan, M. Lachemi, and K. M. A. Hossain, “Effect of metakaolin and silica fume on the durability of self-consolidating concrete,” *Cement and Concrete Composites*, vol. 34, no. 6, pp. 801–807, 2012.

[23] J. Wang, Q. Shen, F. Wang, and W. Wang, “Experimental and analytical studies on CFRP strengthened circular thin-walled CFST stub columns under eccentric compression,” *Thin-Walled Structures*, vol. 127, pp. 102–119, 2018.